Inorg. Chem. **2006**, *45*, 3671–3678

2D and 3D $Cu(hfac)_2$ Complexes with Nitronyl Nitroxide Biradicals

Eugene Tretyakov,[†,‡] Sergei Fokin,[‡] Galina Romanenko,[†] Vladimir Ikorskii,[†] Sergei Vasilevsky,[§] and Victor Ovcharenko*[,†]

International Tomography Center, Siberian Branch of the Russian Academy of Sciences, 630090, Novosibirsk, Russia, Novosibirsk State University, Pirogova str., 2, 630090, Novosibirsk, Russia, and Institute of Chemical Kinetics and Combustion, Siberian Branch of the Russian Academy of Sciences, 630090, Novosibirsk, Russia

Received January 23, 2006

Reactions between $Cu(hfac)_2$ and nitronyl nitroxide biradicals 1,4-bis[4-(4,4,5,5-tetramethyl-3-oxide-1-oxyl-4,5-dihydro-1*H*-imidazol-2-yl)pyrazol-1-yl]butane (**L**^{4}) and 1,8-bis[4-(4,4,5,5-tetramethyl-3-oxide-1-oxyl-4,5-dihydro-1*H*-imidazol-2-yl)pyrazol-1-yl]octane (**L**^{8}) gave respectively a framework compound $[Cu(hfac)_2]_2$**L**^{4} and a layered polymer compound $[Cu(hfac)_2]_2$**L**^{8}. The framework of $[Cu(hfac)_2]_2$**L**^{4} consists of 66-membered condensed metallocycles. Inside the framework, the structure has macrohelixes (pitch ∼25 Å) extending along the [001] crystallographic direction. All the helixes have the same direction of winding; the crystals, therefore, are optically active, the structure corresponding either to *P*-isomer ($P4_12_12$) or to *M*-isomer ($P4_32_12$). The long distances between the Cu atoms and the O atoms of the coordinated >N–O groups (Cu–O 2.351–2.467 Å) are responsible for ferromagnetic exchange interactions in Cu^{2+}–O∴N< and >N∴O–Cu^{2+}–O∴N< exchange clusters.

Introduction

Specific magnetic anomalies were previously found for $Cu(hfac)_2$ complexes with 1-alkylpyrazol-4-yl-substituted nitronyl nitroxides (**L**^{R}, Chart 1), whose temperature dependences of the effective magnetic moment (μ_{eff}) suggested spin transitions.[1,2] In the solid state, all of these complexes are heterospin 1D polymers with "head-to-head" or "head-to-tail" chain motifs, arising from the bridging coordination of **L**^{R} via the O atom of one of the >N−O groups and the N atom of the pyrazole ring. We attempted to examine the possibilities for synthesis of more highly dimensional (2D and 3D) heterospin structures from $Cu(hfac)_2$ complexes with 1-alkylpyrazol-4-yl-substituted nitronyl nitroxides. For construction units capable of provoking higher dimensionality in the complexes, we used biradicals of definite structure, namely, biradicals containing tetra- and octamethylene linking groups between the pyrazole fragments (**L**^{4} and **L**^{8}; the superscript denotes the number of methylene units, Chart 1).

Note that using biradicals for these syntheses does not guarantee the formation of highly dimensional heterospin structures. Thus, the Cambridge Structural Database[3] contains references to 31 structures of transition metal complexes with nitronyl nitroxide and imino nitroxide biradicals,[4] of which only two are chain-polymer structures,[4a,o] while all others are molecular structures in the solid state. Data about 2D and 3D complexes with biradicals are unavailable. Construction of a highly dimensional structure should follow certain requirements. Even if we neglect the hardly predictable kinetic and thermodynamic factors, restricting our analysis to structural complementarity of blocks to be used for assembling highly dimensional structures, we still have a lot of possibilities.[5,6] Therefore, prior to synthesis of $Cu(hfac)_2$ complexes with **L**^{4} and **L**^{8}, we had carried out preliminary structural simulations of possible packings. It was primarily taken into account that the majority of previously synthesized $Cu(hfac)_2$ complexes with **L**^{R} monoradicals preferably had a bridging bidentate paramagnetic ligand, provoking chain formation. For the biradical molecule, the choice of the length

* To whom correspondence should be addressed. E-mail: Victor.Ovcharenko@tomo.nsc.ru.
† International Tomography Center.
‡ Novosibirsk State University.
§ Institute of Chemical Kinetics and Combustion.

(1) Ovcharenko, V. I.; Maryunina, K. Yu.; Fokin, S. V.; Tretyakov, E. V.; Romanenko, G. V.; Ikorskii, V. N. *Russ. Chem. Bull. (Engl. Transl.)* **2004**, 2406.
(2) Rey, P.; Ovcharenko, V. I. Spin Transition Phenomena. In *Magnetism: Molecules to Materials IV*; Miller, J. S., Drillon, M., Eds.; Wiley-VCH: Weinheim, Germany, 2003; p 41.
(3) *Cambridge Structural Database*, version 5.26; Cambridge Crystallographic Data Centre: Cambridge, U.K., November 2004 (updates August 2005).

10.1021/ic060132e CCC: $33.50
Published on Web 04/01/2006

Chart 1

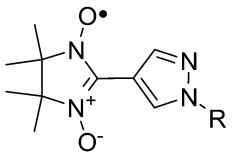

$\mathbf{L^R}$ **(R = Me, Et, *n*-Pr, *i*-Pr, *n*-Bu)**

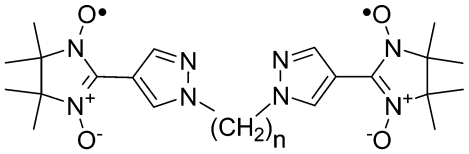

$\mathbf{L^4}$ **(n = 4),** $\mathbf{L^8}$ **(n = 8)**

n of $-(CH_2)_n-$ groups necessary for chain cross-linking was dictated by the data available in our structural database for chain polymers of $Cu(hfac)_2$ with 1-alkylpyrazol-4-yl-substituted nitronyl nitroxides.[1,2] Our simulation showed that in polymer chains with both head-to-head and head-to-tail motifs, pronounced structural strains and distortions are caused by chain linking via polymethylene bridges with less than four methylene units between the pyrazole fragments. According to simulation data, however, more than eight $-(CH_2)-$ units is undesirable because the chain can undergo unpredictable twisting. Therefore, for biradicals we chose derivatives with $n = 4$ and $n = 8$ corresponding to the boundary values. Indeed, we succeeded in obtaining the first layered polymer and framework complexes with the nitronyl nitroxide biradical, whose structures possess a number of nontrivial features.

Results and Discussion

Synthesis of Biradicals. $\mathbf{L^4}$ and $\mathbf{L^8}$ were prepared by alkylating $\mathbf{L^H}$ with 1,4-dibromobutane or 1,8-dibromooctane, respectively (Scheme 1). To generate the sodium salt of spin-labeled pyrazole, we used either aqueous NaOH or a suspension of NaH in DMF, or NaOH and NBu_4Br in an H_2O−benzene heterophase system. These procedures afforded $\mathbf{L^4}$ and $\mathbf{L^8}$ with ∼50−75% yields.

In previous syntheses of 2-imidazoline nitroxides with an *N*-alkylpyrazol-4(3)-yl substituent in the 2 position, the alkyl group was introduced in the pyrazole ring at an early stage

Scheme 1

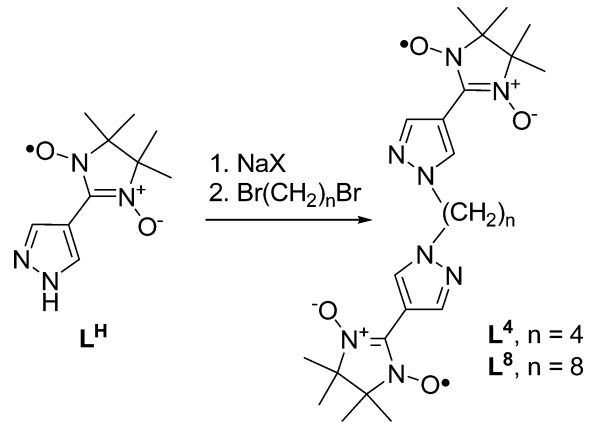

of radical synthesis. In the case of $\mathbf{L^4}$ and $\mathbf{L^8}$, we demonstrated the possibility of alkylating spin-labeled pyrazole $\mathbf{L^H}$ as a new approach to synthesis of nitroxides. The $\mathbf{L^4}$ biradical, as well as its solvates with diethyl ether and methylene chloride ($\mathbf{L^4}\cdot OEt_2$ and $\mathbf{L^4}\cdot CH_2Cl_2$), was grown as X-ray quality single crystals; X-ray analysis confirmed the structure of the products. In the solid state, biradical molecules are Z-like (Figure 1). The intermolecular distances between the O atoms of the nitroxyl groups are at least 4 Å, which leads to weak exchange interactions between the paramagnetic centers (Figure 2).

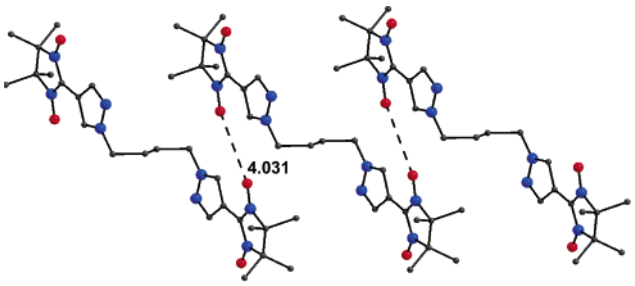

Figure 1. Packing of $\mathbf{L^4}$ molecules: carbon, black; oxygen, red; nitrogen, blue.

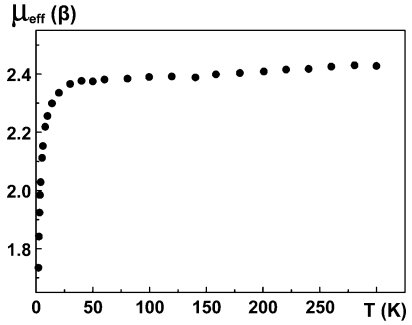

Figure 2. Dependence $\mu_{eff}(T)$ for $\mathbf{L^4}$.

(4) (a) Caneschi, A.; Chiesi, P.; David, L.; Ferraro, F.; Gatteschi, D.; Sessoli, R. *Inorg. Chem.* **1993**, *32*, 1445. (b) Luneau, D.; Laugier, J.; Rey, P.; Ulrich, G.; Ziessel, R.; Legoll, P.; Drillon, M. *Chem. Commun.* **1994**, 741. (c) Caneschi, A.; David, L.; Ferraro, F.; Gatteschi, D.; Fabretti, A. C. *Inorg. Chim. Acta* **1994**, *217*, 7. (d) Oshio, H.; Ohto, A.; Fujisawa, J.; Watanabe, T.; Ito, T.; Isobe, K. *Chem. Lett.* **1994**, 2353. (e) Luneau, D.; Romero, F. M.; Ziessel, R. *Inorg. Chem.* **1998**, *37*, 5078. (f) Romero, F. M.; Luneau, D.; Ziessel, R. *Chem. Commun.* **1998**, 551. (g) Tanaka, M.; Matsuda, K.; Itoh, T.; Iwamura, H. *Angew. Chem., Int. Ed.* **1998**, *37*, 810. (h) Vostrikova, K. E.; Belorizky, E.; Pecaut, J.; Rey P. *Eur. J. Inorg. Chem.* **1999**, 1181. (i) Francese, G.; Romero, F. M.; Neels, A.; Stoeckli-Evans, H.; Decurtins, S. *Inorg. Chem.* **2000**, *39*, 2087. (j) Oshio, H.; Yamamoto, M.; Ito, T. *J. Chem. Soc., Dalton Trans.* **1999**, 2641. (k) Oshio, H.; Yaginuma, T.; Ito, T. *Inorg. Chem.* **1999**, *38*, 2750. (l) Oshio, H.; Yamamoto, M.; Ito, T.; Kawauchi, H.; Koga, N.; Ikoma, T.; Tero-Kubota, S. *Inorg. Chem.* **2001**, *40*, 5518. (m) Zhang, D.; Liu, W.; Xu, W.; Jin, X.; Zhu, D. *Inorg. Chim. Acta* **2001**, *318*, 84. (n) Stroh, C.; Ziessel, R. *Chem. Commun.* **2002**, 1916. (o) Sporer, C.; Wurst, K.; Amabilino, D. B.; Ruiz-Molina, D.; Kopacka, H.; Jaitner, P.; Veciana, J. *Chem. Commun.* **2002**, 2342. (p) Stroh, C.; Belorizky, E.; Turek, P.; Bolvin, H.; Ziessel, R. *Inorg. Chem.* **2003**, *42*, 2938. (q) Fokin, S. V.; Romanenko, G. V.; Baumgarten, M.; Ovcharenko, V. I. *Russ. J. Struct. Chem. (Engl. Transl.)* **2003**, *44*, 864. (r) Zhang, D.; Liu, W.; Shuai, Z.; Hu, H.; Xu, W.; Zhu, D. *Synth. Met.* **2003**, *133*, 601. (s) Ichimura, T.; Doi, K.; Mitsuhashi, C.; Ishida, T.; Nogami, T. *Polyhedron* **2003**, *22*, 2557.
(5) Philp, D.; Stoddart, J. F. *Angew. Chem., Int. Ed. Engl.* **1996**, *35*, 1154.
(6) Moulton, B.; Lu, J.; Zaworotko, M. J. *J. Am. Chem. Soc.* **2001**, *123*, 9224.

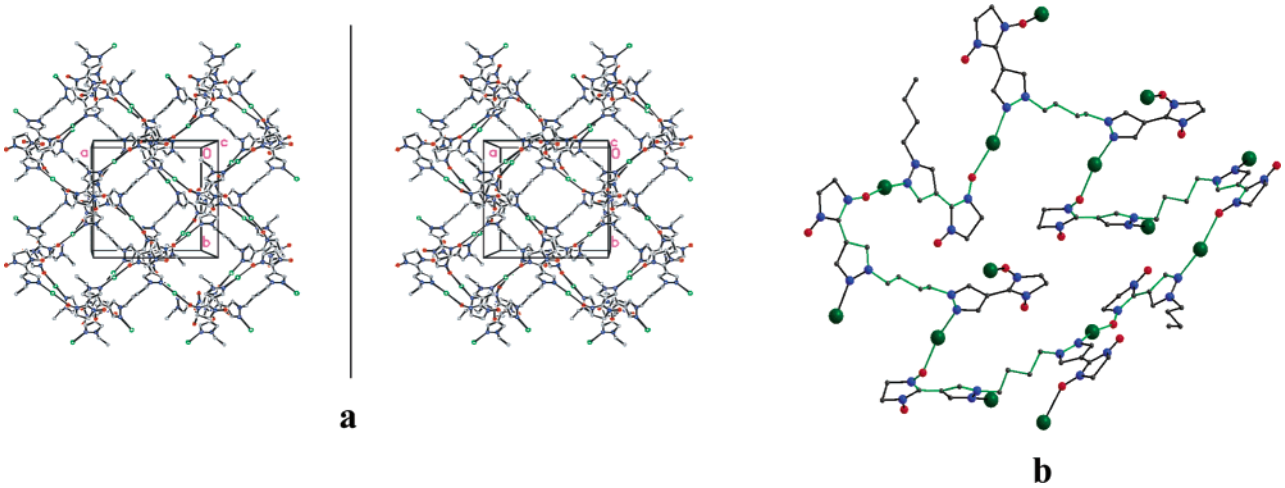

Figure 3. Stereoview of the framework (a) and 66-membered metallocycle (shown as green bonds) in structure **1** (b): copper, deep-green; carbon, black; oxygen, red; nitrogen, blue.

Synthesis and Structure of Complexes. The reactions of Cu(hfac)$_2$ with **L^4** and **L^8** yielded highly dimensional multispin structures. Thus, our spatial simulation that was carried out at an early stage of investigation and indicated the formation of 2D or 3D structures for biradicals with a $-(CH_2)_n-$ polymethylene bridge ($4 \leq n \leq 8$) proved justified. However, the character of the polymer structure varied between Cu(hfac)$_2$ complexes with **L^4** and **L^8**.

Solid [Cu(hfac)$_2$]$_2$**L^4** (**1**) is a framework polymer where each Cu atom coordinates two **L^4** ligands via the O atom of the >N−O group and the pyrazole N atom. The framework is formed from 66-membered (along the shortest perimeter) annelated metallocycles of complex configuration discernible in the stereopair shown in Figure 3a. Figure 3b presents one of the 66-membered rings in a convenient projection to demonstrate that all **L^4** within the framework structure are generally coordinated as tetradentate ligands. For two of six bridging molecules shown in Figure 3b and having tetramethylene fragments involved in other annelated 66-membered rings, only the half-biradical molecule is presented. To avoid overcrowding of the figure, the **L^4** molecules are depicted as each bonded to only two Cu atoms. Further construction in the direction of leaving tetramethylene fragments (shown as black groups in the figure) gives the other half of the biradical also bonded to two Cu atoms.

For easy perception of structure **1**, it is appropriate to isolate a fragment {Cu$_2$**L^4**Cu$_2$} formed by the **L^4** molecule coordinated to four Cu atoms and to approximate the fragment by a distorted tetrahedron with Cu atoms at the vertexes. In this representation, the complex framework of **1** is reduced to a packing of tetrahedra similar to that in cristobalite (Figure 4a). If viewed along the *c* direction perpendicular to the plane of the drawing, all tetrahedra in the packing can be seen as going deep into the structure along the 4-fold screw axis, forming helixes. A fragment of a helix colored yellow is shown in Figure 4b. In this perspective view, the fifth bottom tetrahedron repeats the first top one. Figure 4c gives a simpler representation of structure **1**. The imaginary lines link the centers of gravity of the 66-membered rings, which are also viewed in perspective as

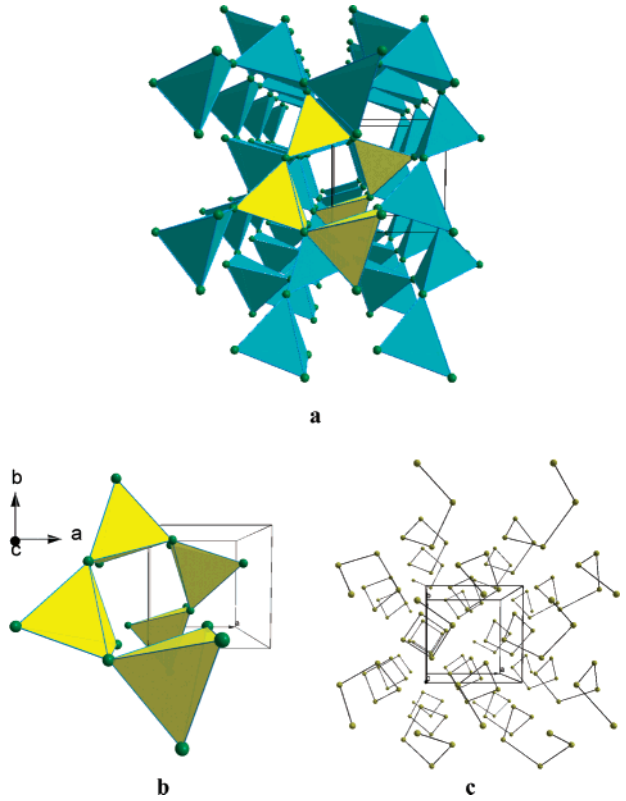

Figure 4. Packing of {Cu$_2$**L^4**Cu$_2$} tetrahedra in structure **1** (a); fragment of a helix of tetrahedra (b); spirals of associated centers of gravity of 66-membered rings (c).

helixes that wind in the same direction. Structure **1** in general proved optically active; the variation of its representation shown in Figure 4c corresponds to the *P*-helixes (space group $P4_12_12$). Crystals with *M*-helixes were also present in the solid phase, as confirmed by an X-ray diffraction study (space group $P4_32_12$).

Finally, if in any 66-membered ring (Figure 3b) the biradical molecule is split into two fragments (Cu−N$_{Pz}$ and Cu−O) at the middle of the $-(CH_2)_4-$ methylene chain, each of these fragments coordinated to the copper ion creates a head-to-tail motif in the coordination sphere of the metal.

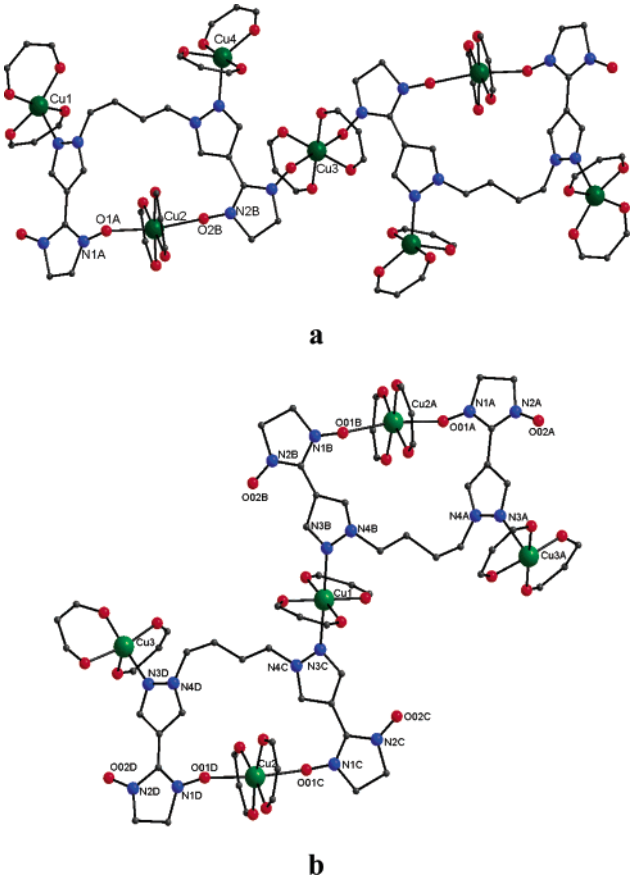

Figure 5. Ball-and-stick diagram of **2** (a) and **3** (b): copper, deep-green; carbon, black; oxygen, red; nitrogen, blue.

The use of acetone/heptane or diethyl ether as a solvent led to the crystallization of **1** irrespective of the initial ratio of $Cu(hfac)_2/\mathbf{L^4}$. The use of benzene/heptane, however, yielded another compound, $[Cu(hfac)_2]_7\mathbf{L^4}_2 \cdot C_6H_6$ (**2**). The composition of **2** indicates that the solid phase is saturated with $Cu(hfac)_2$ matrixes. Therefore, it seemed reasonable to try to obtain this compound from reagent mixtures with a ratio of $Cu(hfac)_2/\mathbf{L^4} \approx 7/2$. However, this ratio of reagents led to the formation of noncrystallizable oil. When the initial ratio of $Cu(hfac)_2/\mathbf{L^4}$ was 2/1, crystals **2** mixed with crystals of excess $\mathbf{L^4}$ were isolated from benzene/heptane. From this mixture of crystals we selected seed crystals **2** and subsequently introduced them in the saturated reaction mixtures where $Cu(hfac)_2/\mathbf{L^4} \approx 7/2$. This technique prevented oil formation and stimulated effective growth of crystals **2** alone (~60−70% yield).

Investigation of structure **2** indicated that the complex has a molecular structure (Figure 5a). In centrosymmetric molecule **2**, both bridging pentadentate biradical molecules are U-like. The Cu2 atoms, coordinating the O atoms of the >N−O groups of the same $\mathbf{L^4}$, lock the U-like molecule into a 17-membered metallocycle. The crystallographically independent Cu1−Cu4 atoms have varying surroundings. The coordination polyhedron is a square bipyramid (which is centrosymmetric for Cu3) for Cu2 and Cu3, distorted square pyramid for Cu1, and trigonal bipyramid for Cu4. In the square bipyramids, the axial positions are occupied by the O atoms of the >N−O groups ($Cu-O_{N-O}$ distances are from 2.351 to 2.465 Å). In the square pyramid of Cu1, the axial position is occupied by the N_{Pz} pyrazole atom ($d_{Cu-N_{Pz}} = 2.220$ Å). In the trigonal bipyramid of Cu4, the O_{hfac} atoms are axial ($d_{Cu-O_{hfac}} = 1.906$ and 1.920 Å), while the N_{Pz} atom lies in the equatorial plane ($d_{Cu-N_{Pz}} = 2.136$ Å).

As is known, stereochemical lability of the metal-containing matrix in a $Cu(hfac)_2$−nitroxide system makes it possible to synthesize a great variety of compounds.[7] Our goal being a reliable procedure for the synthesis of highly dimensional heterospin compounds with $\mathbf{L^4}$ and $\mathbf{L^8}$, we succeeded in readily synthesizing framework compound **1**. Nevertheless, we continued experiments by varying the synthetic conditions (reagent ratio, solvent, temperature) in order to examine the possibility of synthesizing other compounds. In the case of $\mathbf{L^4}$, however, we always obtained crystal **1** or crystal **2**. Occasionally, during synthesis of **1** (see Experimental Section) we obtained prismatically shaped, solitary single crystals of $[Cu(hfac)_2]_5\mathbf{L^4}_2$ (**3**) as an impurity. Sometimes they formed (exclusively on the walls of the flask) when the reaction mixture was quickly concentrated by blowing it with a flow of air. A few high-quality crystals were selected, and the structure of **3** has been determined (Figure 5b). In Figure 5, molecules **2** and **3** are juxtaposed in projections that reveal certain structural similarity between them. Thus, molecule **3** can be mentally derived from molecule **2**. At first, the $Cu^3(hfac)_2$ and $Cu^{4'}(hfac)_2$ fragments can be removed from **2**, and then the coordination sphere of $Cu^4(hfac)_2$ can be completed by binding with the N atom of the pyrazole ring. As in **2**, the $\mathbf{L^4}$ molecules are U-shaped and locked via $Cu(hfac)_2$ matrixes into a 17-membered metallocycle. The Cu1 atom is surrounded by a square bipyramid whose equatorial plane is formed by the O_{hfac} atoms ($d_{Cu-O_{hfac}} = 1.961(7)-1.997(6)$ Å) and whose vertexes are occupied by the N_{Pz} atoms ($d_{Cu-N_{Pz}} = 2.337(8)$ and 2.366(8) Å) of the two $\mathbf{L^4}$ ligands. In the square bipyramids surrounding Cu2 and Cu2A, the axial positions are occupied by the O atoms of the >N−O groups. The $Cu-O_{N-O}$ distances are long enough, from 2.418(6) to 2.513(6) Å. Molecule **3** is noncentrosymmetric. The environment of the terminal Cu3 atom differs substantially from that of the terminal Cu3A atom. For both atoms, the surroundings are distorted square pyramids but Cu3 has the N_{Pz} atom lying at the base of the pyramid ($d_{Cu-N_{Pz}} = 2.068(7)$ Å), while Cu3A has the same atom lying at the apex ($d_{Cu-N_{Pz}} = 2.338(7)$ Å).

The reaction of $Cu(hfac)_2$ with $\mathbf{L^8}$ led to solid $[Cu(hfac)_2]_2\mathbf{L^8}$ (**4**) with a layered polymer structure (Figure 6). Each copper atom has square bipyramidal surroundings. In half of all these bipyramids, the apical positions are occupied by the N_{Pz} atoms and in the other half by the O atoms of the >N−O groups. If division lines (dashed lines in Figure 6) are mentally drawn through the middles of the octamethylene fragments, then structure **4** may be regarded as head-to-head polymer chains formed from $Cu(hfac)_2$ matrixes and bridging nitroxides cross-linked by $-(CH_2)_8-$ units into layers. With this division, the chains found between the dashed lines are identical in their motif to the chains described for Cu-

(7) Fokin, S.; Ovcharenko, V.; Romanenko, G.; Ikorskii, V. *Inorg. Chem.* **2004**, *43*, 969.

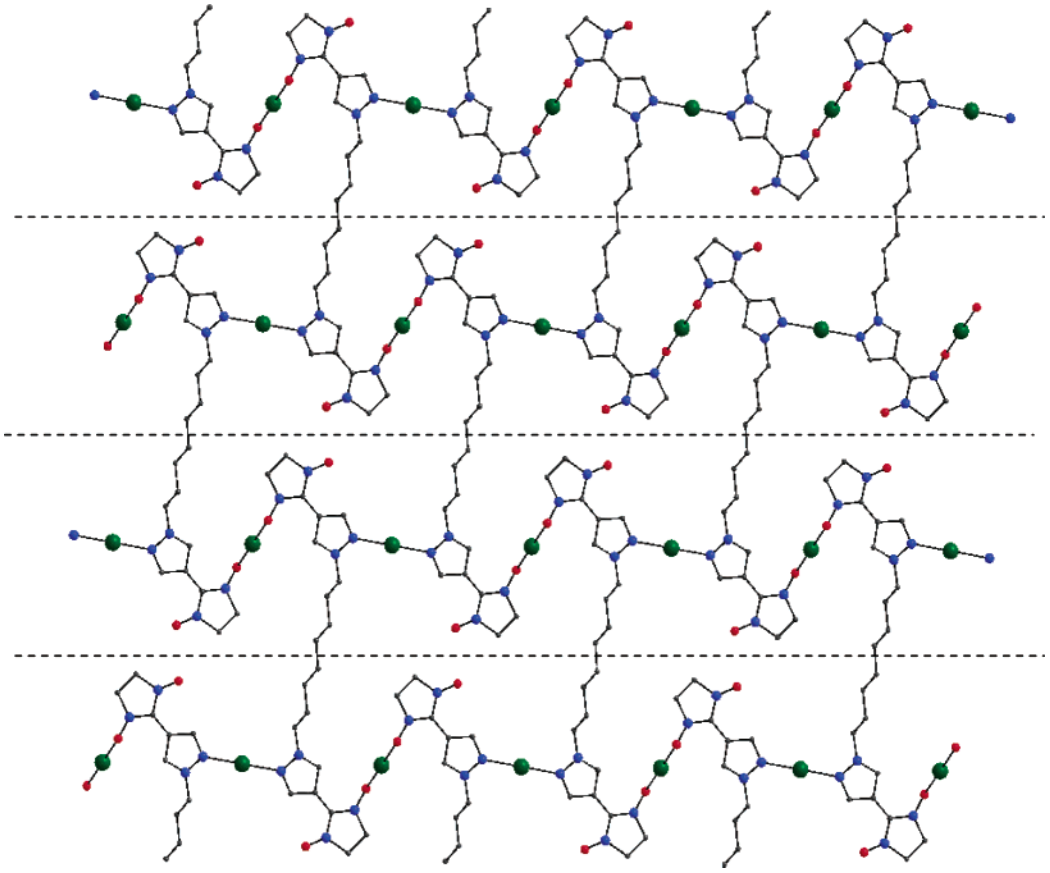

Figure 6. Structure of layer in **4**: copper, deep-green; carbon, black; oxygen, red; nitrogen, blue. The dashed lines reflect the conventional partitioning into chains.

Table 1. Selected Bond Lengths of **1**, **4**, and **5** at Different Temperatures (Å)

	1			**4**			**5**[8]		
	120 K	240 K	295 K	110 K	200 K	295 K	123 K	167 K	295 K
Cu−O_{N-O}	2.454(2)	2.476(3)	2.467(4)	2.432(2)	2.444(3)	2.460(4)	2.006	2.251	2.320
Δd (Cu−O_{N-O})	0.013			0.028			0.314		
Cu−N_{Pz}	2.267(2)	2.270(3)	2.275(4)	2.405(2)	2.392(3)	2.391(4)	2.459	2.469	2.514
Δd (Cu−N_{Pz})	0.008			0.014			0.065		

(hfac)$_2$**L**$^{\mathbf{R}}$ (R = C_2H_5, C_3H_8, C_4H_9), which showed magnetic anomalies.[1,2] Therefore it was reasonable to compare the temperature dependence of the Cu−N_{Pz} and Cu−O_{N-O} bond lengths of this compound with the same dependence of, for example, Cu(hfac)$_2$**L**$^{n\text{-Bu}}$, where the *n*-Bu fragment may be viewed as an analogue of one-half of the **L**$^{\mathbf{8}}$ octamethylene unit. Table 1 shows that at reduced temperatures Δd for Cu−N_{Pz} and Cu−O_{N-O} bond lengths in **4** differs from that in Cu(hfac)$_2$**L**$^{n\text{-Bu}}$ (**5**), which exhibits a structural phase transition and an associated magnetic anomaly (abrupt change in μ_{eff}) at 163 K.[1] For **4**, the values of Δd are much smaller and reflect that the substance undergoes insignificant compression at reduced temperatures.

The same is observed for structure **1** (Table 1). Therefore, 3D and 2D polymers **1** and **4** are more "rigid" solids compared with Cu(hfac)$_2$**L**$^{\mathbf{R}}$ 1D polymers. Compound **1** with a framework structure is a close-packed compound with high enough D_c (1.708 g·cm^{-3} at 295 K, Table 3). For comparison, D_c is 1.435 g·cm^{-3} at 295 K for **5**.[8] In structure **4**, also possessing higher density (1.541 g·cm^{-3} at 295 K, Table 3) compared with that of **5**, the polymer layers have no space for atomic motion. For example, in **4**, the distance between the N atoms linked by −$(CH_2)_8$− fragments is 11.26 Å, which exceeds the theoretical value of 10.58 Å derived by using the typical C−N and C−C distances of 1.48 and 1.54 Å, respectively, and the angles of 109.5° at the C atoms. The stated "rigidity" of structures **1** and **4** obviously hinders the magnetic anomalies observed for Cu(hfac)$_2$**L**$^{\mathbf{R}}$.

Table 2. Optimal Parameters g_{Cu}, J, and $J'z$

parameter	**1**	**2**	**4**
g_{Cu}	2.07 ± 0.02	2.05 ± 0.03	2.07 ± 0.01
J (cm^{-1})	14.7 ± 0.8	30.9 ± 0.2 (J_1) 7.6 ± 0.1 (J_2)	11.2 ± 0.1
nJ' (cm^{-1})	−0.12 ± 0.02	−0.64 ± 0.01	−0.36 ± 0.01

Magnetic Properties. The tetramethylene and octamethylene bridges in **1** and **4** drastically decrease the energies of exchange interactions among Cu^{2+}−O∴N< and >N∴O−Cu^{2+}−O∴N< exchange clusters, respectively, which have internal ferromagnetic exchange interactions (Figure 7, Table

(8) Ovcharenko, V. I.; Fokin, S. V.; Romanenko, G. V.; Ikorskii, V. N.; Tretyakov, E. V.; Vasilevsky, S. F.; Sagdeev, R. Z. *Mol. Phys.* **2002**, *100*, 1107.

Table 3. Crystal Data for **1**−**4**

structure params	(*P*)-**1**	(*P*)-**1**	(*P*)-**1**	(*M*)-**1**	**2**	**3**	**4**	**4**	**4**
empirical formula	$C_{22}H_{20}CuF_{12}N_4O_6$				$C_{124}H_{92}Cu_7F_{84}N_{16}O_{36}$	$C_{98}H_{82}Cu_5F_{60}N_{16}O_{28}$	$C_{48}H_{48}Cu_2F_{24}N_8O_{12}$		
fw	727.96	727.96	727.96	727.96	4422.92	3389.50	1530.04	1530.04	1530.04
space group	$P4_12_12$	$P4_12_12$	$P4_12_12$	$P4_32_12$	$P\bar{1}$	$P1$	$P\bar{1}$	$P\bar{1}$	$P\bar{1}$
Z	8	8	8	8	1	1	1	1	1
T (K)	120	240	295	295	295	295	110	200	295
a (Å)	14.9346(7)	15.095(1)	15.089(2)	15.2040(8)	11.0531(6)	12.458(2)	11.276(4)	11.281(3)	11.314(3)
b (Å)	14.9346(7)	15.095(1)	15.089(2)	15.2040(8)	14.9148(8)	16.387(3)	11.488(5)	11.598(4)	11.817(3)
c (Å)	24.800(2)	24.850(3)	24.861(8)	24.909(2)	27.864(1)	19.262(4)	13.795(5)	13.742(4)	13.746(4)
α (deg)					104.549(1)	105.290(3)	92.934(7)	93.574(6)	94.706(5)
β (deg)					93.670(1)	103.114(3)	114.139(7)	113.391(6)	111.839(5)
γ (deg)					90.008(1)	107.368(3)	103.139(7)	103.059(5)	103.492(5)
V (Å^3)	5531.4(6)	5662.6(9)	5660(2)	5758.0(6)	4436.4(4)	3414.8(11)	1567.0(11)	1584.0(8)	1629.5(8)
D_{calcd} (g·cm^{-3})	1.748	1.708	1.708	1.679	1.655	1.648	1.619	1.604	1.541
μ (mm^{-1})	0.916	0.895	0.896	0.880	0.982	0.919	0.814	0.805	0.781
θ (deg)	1.59−23.27	1.91−23.29	1.91−23.25	1.89−23.30	2.04−23.29	1.80−23.32	1.84−23.28	1.64−23.33	2.02−23.25
I_{hkl} (measd/unique)	24085/3979	24708/4086	24791/4076	42895/4145	19444/12707	24848/18416	6759/4469	6921/4538	7096/4647
R_{int}	0.0406	0.0443	0.0646	0.0811	0.0435	0.0370	0.0521	0.0677	0.0743
N	477	477	477	505	1404	1945	537	537	528
GOF	0.976	1.160	0.854	0.893	0.883	1.001	0.809	0.908	0.958
R_1[a]	0.0269	0.0370	0.0428	0.0363	0.0593	0.0953	0.0382	0.0463	0.0615
wR2 ($I > 2\sigma_I$)	0.0719	0.0945	0.0904	0.0844	0.1458	0.2497	0.0987	0.1208	0.1496
R_1	0.0280	0.0399	0.0555	0.0437	0.0979	0.1607	0.0475	0.0593	0.0923
wR2 (all data)	0.0725	0.0961	0.0959	0.0875	0.1633	0.3215	0.1020	0.1250	0.1647

[a] wR2 = $\{\sum[w(F_o^2 - F_c^2)^2]/\sum[w(F_o^2)^2]\}^{1/2}$ and $R_1 = \sum||F_o| - |F_c||/\sum|F_o|$. The weight scheme employed was $w = 1/[\sigma^2(F_o^2) + (aP)^2 + bP]$ and $P = [2F_c^2 + \max(F_o^2,0)]/3$.

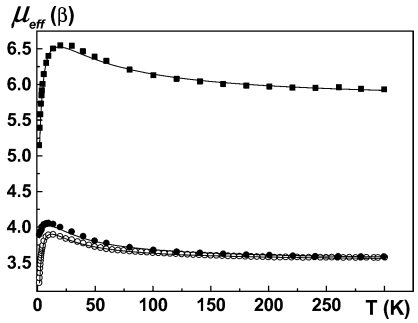

Figure 7. Experimental dependences $\mu_{eff}(T)$ for **1** (○), **2** (■), and **4** (●). The solid lines are theoretical curves with corresponding optimal parameters presented in Table 2.

2). At ambient temperatures, μ_{eff} is 3.58 β and 3.57 β for **1** and **4**, respectively, and approximates the theoretical value of 3.46 β for four practically noninteracting spins $s = {}^1/_2$ with $g = 2$ (β is the Bohr magneton). For **2**, μ_{eff} is 5.93 β, which is also close to the theoretical value of 5.74 β, corresponding to a system of 11 weakly interacting centers with $s = {}^1/_2$ and $g = 2$. At lower temperatures, μ_{eff} increases for **1**, **2**, and **4**, which points to predominant ferromagnetic exchange interactions between the paramagnetic centers in quasi-isolated $Cu^{2+}-O\dot{-}N<$ and $>N\dot{-}O-Cu^{2+}-O-N<$ exchange clusters. Below 10−15 K, μ_{eff} decreases because of weaker antiferromagnetic intercluster exchange interactions.

The exchange structure may be regarded as a system of practically isolated two-center exchange clusters ($Cu^{2+}-O\dot{-}N<$) for **1**, as a system of practically isolated three-center exchange clusters ($>N\dot{-}O-Cu^{2+}-O\dot{-}N<$) and isolated Cu(II) ions lying in CuN_2O_4 coordination polyhedra for **4**, and as a system of practically isolated seven-center clusters ($>N\dot{-}O-Cu^{2+}-O\dot{-}N-C{=}N{\rightarrow}O-Cu^{2+}-O{\leftarrow}N{=}C-N\dot{-}O-Cu^{2+}-O\dot{-}N<$) and four isolated terminal Cu(II) ions lying in the $CuNO_4$ polyhedra (Chart 2) for **2**.

Chart 2

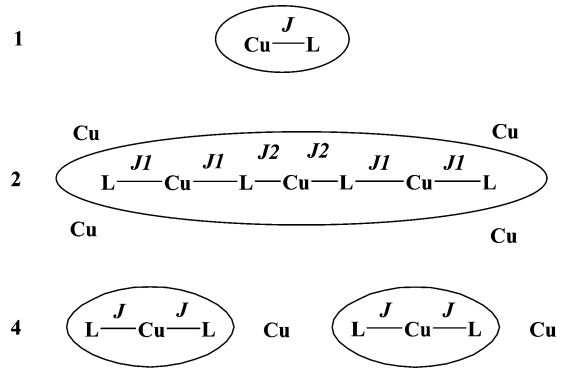

The dependences $\mu_{eff}(T)$ for **1**, **2**, and **4** were analyzed in a cluster approximation using isotropic spin Hamiltonian $\hat{H} = -2\sum_{i,j} J_{ij}\hat{s}_i\hat{s}_j$ within the framework of the approach described elsewhere.[9] To describe the dependence $\mu_{eff}(T)$ for **2**, the g factors were taken to be equal for all Cu(II) ions to avoid reparametrization of the problem despite the slightly different surroundings of the ions. Table 2 lists the optimal parameters of the effective g factor of the copper ion (g_{Cu}), exchange interactions (J), and intercluster exchange interactions (nJ').

As can be seen in Figure 7, the theoretical curves nicely approximate the experimental dependences $\mu_{eff}(T)$ for **1**, **2**, and **4**. They point to ferromagnetic spin interactions in $Cu^{2+}-O\dot{-}N<$ and $>N\dot{-}O-Cu^{2+}-O\dot{-}N<$ exchange clusters. The $Cu-O_{N-O}$ distances being long enough (2.351−2.467 Å) in **1**, **2**, and **4**, ferromagnetic exchange in these exchange clusters is fully consistent with quantum-chemical predictions for these systems.[10]

(9) Ovcharenko, I. V.; Shvedenkov, Y. G.; Musin, R. N.; Ikorskii, V. N. *Russ. J. Struct. Chem. (Engl. Transl.)* **1999**, *40*, 29.

Conclusions

Thus, we have attempted to examine the possibilities for synthesis of highly dimensional heterospin structures from Cu(hfac)$_2$ complexes with 1-alkylpyrazol-4-yl-substituted nitronyl nitroxides. For this purpose, **L^4** and **L^8** biradicals with tetra- and octamethylene linking groups between the pyrazole fragments were used as construction elements capable of provoking an increase in dimensionality. Indeed, we succeeded in obtaining layered polymer and framework complexes with nitronyl nitroxide biradicals. It appeared, however, that the $-(CH_2)_4-$ and $-(CH_2)_8-$ methylene bridges chosen for biradicals led to the formation of rigid structures that exhibited less dynamics in variation of bond lengths in heterospin exchange clusters compared to previously studied chain polymer complexes.[1]

As mentioned in the Introduction, in both cases (**L^4** and **L^8**) we planned to obtain 2D structures (similar to the one depicted in Figure 6) capable of exhibiting magnetic anomalies previously found for Cu(hfac)$_2$ complexes with 1-alkylpyrazol-4-yl-substituted nitronyl nitroxides, whose temperature dependences of the effective magnetic moment suggested spin transitions. If **L^4** and **L^8** had really formed isostructural motifs when interacting with Cu(hfac)$_2$, we would have been able to compare the temperature dynamics of bond lengths in coordination polyhedra with the spatial characteristics of the $-(CH_2)_4-$ and $-(CH_2)_8-$ groups to judge which of these groups favors the magnetic anomaly. It appeared, however, that reactions of **L^4** and **L^8** with Cu(hfac)$_2$ under similar synthetic conditions led to solids with absolutely different structures. This correlates with the above-mentioned fact that data on heterospin compounds with nitroxide biradicals are too scarce to make reliable structural predictions, especially because the use of biradicals in synthesis does not ensure the formation of highly dimensional heterospin structures. It is not accidental, therefore, that of more than 30 documents in the Cambridge Structural Database[3] with structural data on transition metal complexes with nitronyl nitroxide and imino nitroxide biradicals, only two report solids with a polymer chain structure.[4a,o] The layered polymer compound **4** and the framework compound **1** described here should be added to this class of polymer complexes. All other compounds have a molecular structure. Our comparison of the dynamics of bond length variation with temperature (Table 1) for solids **4** and **5** revealed that the structure of **4** is much more rigid than that of **5**, because layered polymer **4** fails to show magnetic anomalies similar to those previously observed for Cu(hfac)$_2$ complexes with pyrazole-substituted mono(nitronyl nitroxides).[1] Further addition of methylene links (>8) will probably fail to eliminate this structural rigidity of the layered polymer (Figure 6, Table 1), which hinders bond length dynamics induced by a variation of temperature.

The unusual structure of optically active framework compound **1** is of particular interest. According to our knowledge, this is the first report of optically active frameworks formed from optically inactive precursors for nitroxide complexes. On the basis of the results of this study, one can assume that optically active framework structures may be found among analogues of **L^4** and **L^8**, in which the index *n* for methylene links between the pyrazole rings in the $-(CH_2)_n-$ fragment is 5−7. Moreover, the possibility of these optically active structures formed in synthesis should be taken into account when planning syntheses of heterospin complexes with polyfunctional nitronyl nitroxides.

Experimental Section

During synthesis of **L^4** and **L^8** the reaction was monitored by TLC using Silufol UV-254 plates. IR spectra of the compounds were recorded on a Bruker IFS 66 spectrometer in KBr.

1,4-Bis[4-(4,4,5,5-tetramethyl-3-oxide-1-oxyl-4,5-dihydro-1*H*-imidazol-2-yl)pyrazol-1-yl]butane (L^4). Procedure 1. 1,4-Dibromobutane (300 mg, 1.39 mmol) was added to a solution of 4,4,5,5-tetramethyl-2-(pyrazol-4-yl)-4,5-dihydro-1*H*-imidazole-3-oxide-1-oxyl[11] (**L^H**) (480 mg, 2.15 mmol) in 40% aqueous NaOH (8 mL). The reaction mixture was stirred at 50−55 °C for 4 h and then for another 2 h at 80−90 °C. After the reaction mixture had been cooled, the product was extracted with $CHCl_3$ (2 × 10 mL). The organic extracts were consolidated, dried over Na_2SO_4, and filtered. The filtrate was evaporated to dryness on a rotary evaporator. The residue was purified by column chromatography using "silica gel 60 (0.063−0.200 mm) for column chromatography" (Merck, column diameter 1.5 cm, column height 10 cm; ethyl acetate as eluent), and a blue fraction containing a compound with $R_f = 0.1$ was collected (for the starting **L^H**, R_f is 0.2). The solvent was distilled off, and the residue was recrystallized from a (1:2) benzene/hexane mixture. The dark blue needle crystals were filtered off and dried in air. Yield 400 mg (75%), mp 175−177 °C. IR spectrum (KBr), ν/cm^{-1}: 649, 672, 753, 817, 870, 972, 1016, 1126, 1187, 1219, 1313, 1352, 1401, 1428, 1458, 1602, 2945, 2993, 3141. Anal. Calcd (%) for $C_{24}H_{36}N_8O_4$: C, 57.6; H, 7.3; N, 22.4. Found (%): C, 57.5; H, 7.2; N, 22.0. Perfect crystals of **L^4** suitable for an X-ray analysis were grown from a toluene/heptane mixture. For an **L^4** single crystal, μ_{eff} is 2.45 β at room temperature, which corresponds to the theoretical value of the magnetic moment for the biradical (Figure 2).

Procedure 2. NaH (22 mg, 60% in mineral oil) was added with stirring to a solution of **L^H** (120 mg, 0.54 mmol) in DMF (5 mL). After 20 min, 1,4-dibromobutane (54 mg, 0.25 mmol) was added to the reaction mixture, and the mixture was stirred at 60−70 °C for 2 h. The solvent was distilled off, and the product was purified as described in Procedure 1. Yield 49 mg (40%).

Synthesis of 1,8-Bis[4-(4,4,5,5-tetramethyl-3-oxide-1-oxyl-4,5-dihydro-1*H*-imidazol-2-yl)pyrazol-1-yl]octane (L^8). A mixture of **L^H** (0.44 g, 1.97 mmol), 1,8-dibromooctae (0.27 g, 0.985 mmol), NBu_4Br (50 mg, 0.16 mmol), NaOH (80 mg, 2 mmol), benzene (5 mL), and water (3 mL) was stirred at 45 °C for 11 h. The reaction mixture was treated with $CHCl_3$ (3 × 15 mL). The organic extracts were consolidated, dried over Na_2SO_4, and filtered; the filtrate was evaporated in a vacuum. The residue (0.55 g) was purified by chromatography on Al_2O_3 (II active; column diameter 2.5 cm, column height 15 cm; $CHCl_3$/ethyl acetate (2:1) as eluent). After

(10) (a) Lanfranc de Panthou, F.; Belorizky, E.; Calemczuk, R.; Luneau, D.; Marcenat, C.; Ressouche, E.; Turek, P.; Rey, P. *J. Am. Chem. Soc.* **1995**, *117*, 11247. (b) Lanfranc de Panthou, F.; Luneau, D.; Musin, R.; Öhrström, L.; Grand, A.; Turek, P.; Rey, P. *Inorg. Chem.* **1996**, *35*, 3484. (c) Musin, R. N.; Ovcharenko, I. V.; Öhrström, L.; Rey, P. *Russ. J. Struct. Chem. (Engl. Transl.)* **1997**, *38*, 711.

(11) Catala, L.; Feher, R.; Amabilino, D. B.; Wurst, K.; Veciana, J. *Polyhedron* **2001**, *20*, 1563.

the solvents had been distilled off, the dark blue residue was ground with 20 mL of hexane. The product was filtered off and recrystallized from a benzene/hexane mixture. Yield 0.37 g (65%), dark blue crystals, mp 137−138 °C. Anal. Calcd (%) for $C_{28}H_{44}N_8O_4$: C, 60.4; H, 8.0; N, 20.1. Found (%): C, 60.2; H, 8.3; N, 19.8.

[Cu(hfac)$_2$]$_2$L^4 (1). A mixture of Cu(hfac)$_2$ (143 mg, 0.3 mmol) and **L^4** (50 mg, 0.1 mmol) was dissolved in acetone (2 mL). Then heptane (5 mL) was added, and the solution was allowed to stay in an open flask for 1 day at room temperature. The resulting octahedral dark blue crystals were filtered off, washed with ether, and dried in air. Yield 60%. Anal. Calcd (%) for $C_{44}H_{40}N_8O_{12}F_{24}Cu_2$: C, 36.3; H, 2.8; N, 7.7; F, 31.3. Found (%): C, 37.0; H, 2.6; N, 7.3; F, 30.1. This complex is also formed when diethyl ether is used as solvent at any reagent ratio. When the reaction mixture was quickly concentrated by blowing it round with a flow of air, solitary prismatic crystals of [Cu(hfac)$_2$]$_5$**L^4**$_2$ (**3**) formed as an impurity on the walls of the flask; their structure has been investigated.

[Cu(hfac)$_2$]$_7$L^4$_2$·C$_6$H$_6$ (2). A mixture of Cu(hfac)$_2$ (47.7 mg, 0.1 mmol) and **L^4** (25 mg, 0.05 mmol) was dissolved in benzene (5 mL). Heptane (2 mL) was added to the resulting dark brown solution. After a few hours, a mixture of crystals **2** and **L^4** formed; they were filtered off, washed with heptane, and dried in air. Crystals **2** were picked from the resulting mixture; then mixtures of Cu(hfac)$_2$ (83.5 mg, 0.17 mmol) and **L^4** (25 mg, 0.05 mmol) in benzene (1 mL) and heptane (4 mL) were added as seeds to the solutions. After a few hours, dark blue crystals **2** were filtered off, washed with cold benzene, and dried in air. Yield 67%. Anal. Calcd (%) for $C_{124}H_{92}N_{16}O_{36}F_{84}Cu_7$: C, 33.7; H, 2.1; N, 5.1; F, 36.1. Found (%): C, 33.9; H, 1.9; N, 4.9; F, 35.2.

[Cu(hfac)$_2$]$_2$L^8 (4). A mixture of Cu(hfac)$_2$ (85.8 mg, 0.18 mmol) and **L^8** (50 mg, 0.09 mmol) was dissolved in diethyl ether (10 mL), and the solution was kept in an open flask at room temperature. After a few hours, claret red crystals formed, which were filtered off, washed with an ether/hexane mixture and then with pure hexane, and dried in air. Yield 40%. Anal. Calcd for $C_{48}H_{48}N_8O_{12}F_{24}Cu_2$ (%): C, 38.1; H, 3.2; N, 7.4; F, 30.2. Found (%): C, 38.2; H, 3.0; N, 7.3; F, 29.1.

X-ray Crystallography. Single-crystal data for the compounds were obtained on a SMART APEX (Bruker AXS) diffractometer with CCD-detector (Mo Kα radiation, $\lambda = 0.71073$ Å, graphite monochromator, 50 kV, 40 mA, $\omega/2\theta$ scan technique, frame width 0.3°) using the standard software (SMART, SAINT).[12,13] Structure solution and refinement were fulfilled using SXTL software.[13] For **L^4**, **L^4**·OEt$_2$, and **L^4**·CH$_2$Cl$_2$, the structural parameters are given as Supporting Information. Crystal data and experimental details are given in Table 3 for **1**−**4**.

Magnetic Measurements. The magnetochemical experiment was run on an MPMS-5S ("Quantum Design") SQUID magnetometer at temperatures from 2 to 300 K in a homogeneous external magnetic field of 5 kOe. Molar magnetic susceptibility χ of the complexes was calculated by using Pascal's additive scheme including diamagnetic corrections and taking into account temperature-independent paramagnetism of Cu(II) ions, which was taken to be 60×10^{-6} cm^3/mol. The effective magnetic moment was calculated by the formula $\mu_{eff} = [(3k/(N_A\beta^2))\chi T]^{1/2} \approx (8\chi T)^{1/2}$, where k is Boltzmann's constant, N_A is the Avogadro number, and β is the Bohr magneton.

Acknowledgment. We are grateful to RFBR (Grants 05-03-32305, 04-03-08002, and 06-03-32157), RFBR-DFG (Grant 06-03-04000), CRDF (Grant Y1-C-08-03), Presidium of RAS, SB RAS, Bruker Company, and the Russian Science Fund for financial support.

Supporting Information Available: Structural determination parameters, crystal and structure refinement data, atomic coordinates, and isotropic displacement parameters for **L^4**, **L^4**·OEt$_2$, **L^4**·CH$_2$Cl$_2$, and **1**−**4** (in CIF format). This material is available free of charge via the Internet at http://pubs.acs.org.

IC060132E

(12) *SMART*, version 5.625; Bruker AXS: Madison, WI, 2001.
(13) *SAINT*, version 6.22; Bruker AXS: Madison, WI, 2001.
(14) Sheldrick, G. M. *SHELX97*, release 97-2; University of Göttingen: Göttingen, Germany, 1998.